Intrinsic kinetics fluctuations as cause of growth inhomogeneity in protein crystals

Peter G. Vekilov* and Franz Rosenberger
Center for Microgravity and Materials Research, University of Alabama in Huntsville, Huntsville, Alabama 35899
(Received 3 December 1997; revised manuscript received 3 February 1998)

Intrinsic kinetics instabilities in the form of growth step bunching during the crystallization of the protein lysozyme from solution were characterized by *in situ* high-resolution optical interferometry. Compositional variations (striations) in the crystal, which potentially decrease its utility, e.g., for molecular structure studies by diffraction methods, were visualized by polarized light reflection microscopy. A spatiotemporal correlation was established between the sequence of moving step bunches and the striations. [S1063-651X(98)03206-1]

PACS number(s): 87.90.+y, 81.10.Aj, 61.72.Cc, 68.35.Ct

Protein crystals are predominantly used for determinations of the molecular structures by x-ray, neutron, or electron diffraction. Three-dimensional structure details at atomic resolution are the key to the understanding of interactions between enzymes and substrates or inhibitors, correlations between genome and protein sequences, rational drug design, and many other problems of biomedical significance [1]. Recent advances in beam and detector technology and in computational crystallography, greatly accelerated high-resolution diffraction studies. Thus the preparation of diffraction-quality crystals has emerged as the bottleneck of macromolecular structure studies [1]. As a consequence, much effort has been spent to gain an understanding of the mechanisms underlying protein crystal growth and the associated formation of compositional and structural defects [2]. Unsteady conditions during growth [3,4], as well as the incorporation of impurities [4–6] and crystallites or amorphous clusters into growing crystals [7], have been shown to degrade the crystals' perfection and thus limit their suitability for diffraction studies. In this paper we show that even if it were possible to eliminate these extrinsic, detrimental factors, protein crystal inhomogeneities can arise from intrinsic instabilities that originate in the coupling of solute transport to the interface with the nonlinear interfacial attachment kinetics.

In earlier work with the model protein lysozyme, we found that under steady solution conditions the locally measured growth rate and growth step density can fluctuate by up to several times their average values [8,9]. The variations in step density reveal that this unsteadiness occurs through the dynamic formation of step bunches. In analogy to various observations with inorganic systems [10,11], we inferred that these kinetic fluctuations represent an intrinsic instability [12] of the growth process under mixed surface-kinetics and bulk-transport control. We tested this supposition by numerical simulations of the diffusive transport and coupled incorporation into individual steps on a growing crystal face [13]. These simulations yielded fluctuations and step bunching of magnitudes and time scales consistent with those observed experimentally. From these results we obtained a system-dependent rationale for the advantages, as well as the disadvantages of specific choices of transport conditions for (protein) crystal perfection.

In this earlier work we also showed that the spacing between striations (bands of inhomogeneities) detected in the crystals was comparable to the thickness of the layers grown between major growth rate excursions, i.e., between the passage of major step bunches at a given location on the interface [9]. Hence we tentatively concluded that these striae originate at step bunches. However, a direct spatiotemporal correlation between growth rate fluctuations, step bunching, and striations in the crystals, similar to that found in semiconductor crystallization [14], remained to be established. In this paper we provide the missing correlation.

The experimental procedures, interferometric data collection, and computer imaging used here have been described before [8]. They allow monitoring (with a depth resolution $\leqslant 200$ Å) of the normal growth rate R, and local vicinal slope p (proportional to the step density), at select locations on the growing facet. The crystallization and solution circulation system was the same as in our forced solution flow studies [15]. The solutions contained 50 mg/ml lysozyme, 2.5 gr/100 ml solution NaCl as a precipitant and 0.05M sodium acetate-acetic acid buffer to fix the pH at 4.5. Since lower solution purity enhances the visibility of striations [5], we used protein as obtained from Seikagaku, which contains ~1 wt. % of the dry protein each of covalent lysozyme dimer and an unidentified protein with a molecular weight of ~19 000 [16,17]. During the growth kinetics monitoring, the solution temperature was stabilized to within 0.01 °C.

A few crystals were nucleated on a horizontal glass plate in a growth cell [15] on our microscopy setup [8]. After some growth at 21 °C, we selected one of the (110) faces for interferometric growth morphology and kinetics monitoring. To mark to beginning of the interferometric data collection, we lowered the temperature by 1 °C to create an interface-delineating striation [3,5]. After 1.5 h of further growth, the data collection was terminated and the temperature was raised to 21 °C to mark the new interface position with a stria. For the visualization of striae, i.e., microscopically thin layers of defects, viewing parallel to the interface is required. For this, the cell was opened and the glass plate was turned vertically. To avoid solution evaporation and optical distortions from curved liquid-air surfaces, the cell was closed and

*Author to whom correspondence should be addressed. FAX: (256) 890-6791. Electronic address: peter@cmmr.uah.edu

 © 1998 The American Physical Society

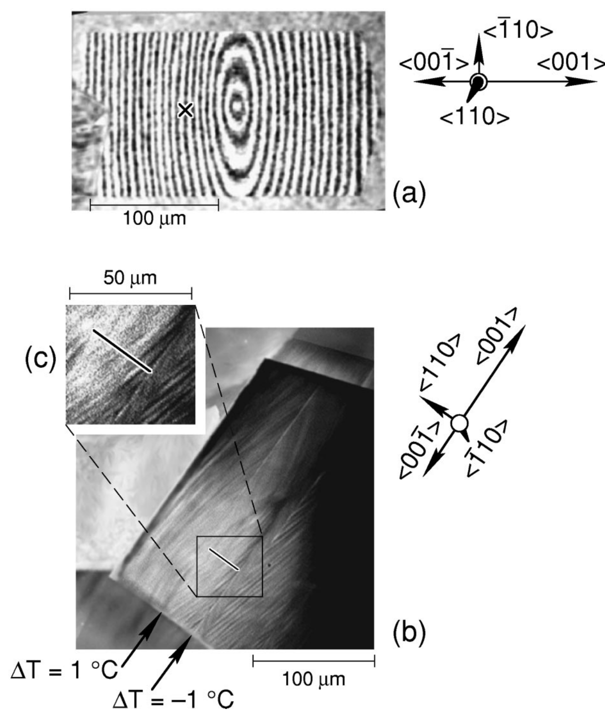

FIG. 1. (a) Interferogram of a (110) face of lysozyme showing a growth hillock at the facet center; for crystallographic directions see the sketch on the right. × marks the location of interferometric monitoring. (b) Polarized light reflection image of the crystal viewed in the direction perpendicular to the direction of observation in (a), with the focal plane positioned in about the middle of the crystal. (c) 2:1 enlargement of the squared area in (b) with enhanced contrast to better visualize the striations. Lines in (b) and (c) correspond to crystal growth during the interferometric monitoring period. Arrows in (b) point to striations caused by $|\Delta T| = 1$ °C before and after monitoring. The orientations of crystallographic axes in (b) and (c) are shown on the right.

filled again with solution. Microscopic striae distribution measurements were then made with reflected polarized light.

Figure 1(a) depicts the interface morphology during the R and p monitoring (Fig. 2) in the form of a top-view interferometric micrograph. In this view, the concentric interference fringes represent the contour lines of the surface morphology [8]. This interferogram indicates that the growth steps are generated at the facet center and spread toward the facet edges, forming a vicinal hillock on the face. The elongated shape of the face and the anisotropy of step velocity (slowest directions [001]) determine the hillock shape shown in this figure. Note that most of the facet is covered by steps moving in the opposite $\langle 001 \rangle$ and $\langle 00\bar{1} \rangle$ directions.

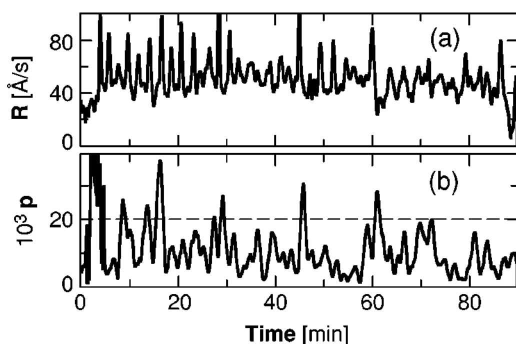

FIG. 2. Time traces of the (a) growth rate R and (b) vicinal slope p recorded at the location marked with × in Fig. 1(a) at $\sigma = 1.9$ ($T = 20$ °C).

Figure 1(b) presents a polarized light micrograph of the grown crystal viewed parallel to the interface. In this side view, the two straight striations that resulted from the imposed temperature changes mark the beginning and end of the monitoring period. In this low-resolution view, these markers appear parallel to the (110) plane. Between the markers, in the lower left region, one can discern a system of closely spaced, inclined striations. The inclination with respect to the (110) plane is between 10° and 15°. A similar system of striations [less clearly discernable with the contrast settings selected for Fig. 1(b)] forms essentially a mirror image of the first set about the (001) plane. The origin and orientation of these sets of striations are compatible with traces left by step bunches on opposite sides of the growth hillock; see above.

Striae originating at macrosteps should be inclined with respect to the singular plane by an angle α, which is related to the *local* normal growth rate R and step bunch velocity v_{bunch} by

$$\tan \alpha = R/v_{\mathrm{bunch}}. \tag{1}$$

By comparing Figs. 2(a) and 2(b), we see that in a bunch (period of maximum p) $R \sim 60$ Å/s. From a comparison of two traces of the vicinal slope $p(t)$ recorded in adjacent pairs of pixels at the monitoring location (for details see Ref. [8]) we obtained $v_{\mathrm{bunch}} \approx 2.5 \times 10^{-6}$ cm/s. Thus Eq. (1) yields $\alpha \approx 14°$, well within the range extracted from Fig. 1(b).

For further evaluation we use the image contained in the square in Fig. 1(b), which is shown in enlarged form in Fig. 1(c), with the black line in both indicating the 32-μm displacement of the interferometric observation location during the measurement period, i.e., between the two markers. Note that about six striations cross this line of growth between the markers in Figs. 1(b) and 1(c) with an average spacing Δx of 5–6 μm. This number equals the number of step bunches with slope greater than 2×10^{-2} in Fig. 2(b). Furthermore, note that the heavier striations at the beginning of the monitoring interval correspond to steeper step bunches.

A more quantitative correlation between the optical image of the striations and the $p(t)$ trace is hampered by the nonlinearities involved in the striation imaging process in Figs. 1(b) and 1(c). Furthermore, the step orientation, density, and number in the step bunches may vary in the $\langle \bar{1}10 \rangle$ direction, perpendicular to the step motion direction (for examples of such step patterns see [14]). This would lead to variations in the optical thickness of the trailing striations, whose projection on the $(\bar{1}10)$ plane is visualized in Figs. 1(b) and 1(c).

Yet, based on the above material, we can clearly correlate the formation of compositional inhomogeneities in lysozyme crystals grown under steady solution conditions with the intrinsic instabilities of layer growth dynamics occurring in the mixed kinetics-bulk transport control regime. Fortunately, based on the dependence of the amplitude of these fluctuations on the ''working point'' (relative weight of transport and kinetics in overall rate control) [9], one can expect that

shifts of the crystallization conditions towards pure kinetics or transport control should result in more steady growth. Depending on the specific system, i.e., its working point, such a shift towards more steady intrinsic conditions may require either enhanced or quiescent (purely diffusive) bulk transport conditions.

From this rationale, it is not surprising that the crystallization of some proteins under reduced gravity (more quiescent transport conditions) has resulted in crystals that diffract to higher resolution, while others did not benefit or showed even lower perfection than their Earth-grown counterparts [9,18]. It may not be obvious how inhomogeneities on the micrometer scale may affect the diffraction resolution obtainable from a crystal in the sub-3-Å range. For this, it is important to note that the maximum diffraction resolution is determined by the signal-to-noise ratio of high-index reflections. Since high-index crystal planes have low molecular density, much wider areas of rotationally and translationally aligned molecules are needed to enhance the intensity of the reflections from these planes and increase their signal-to-noise ratios. Hence crystal imperfections on the scale of micrometers (e.g., striations discussed here) and even tens and hundreds of micrometer (block structures, twins, etc.) affect the diffraction resolution obtainable from a crystal.

Note that lysozyme crystallization from unstirred solutions operates near kinetics control. Thus a reduction of the above step bunching instability should only be expected under enhanced bulk transport conditions. Most recently, we have confirmed this in crystallization experiments with forced solution flow [15,19]. A quantitative account of this increased kinetics stability under enhanced bulk transport is given elsewhere [20].

We thank A. A. Chernov for helpful suggestions. L. Carver expertly prepared the figures. This work was supported by the Microgravity Science and Applications Division of NASA (Grants Nos. NAG8-950 and NAG8-1168) and by the State of Alabama through the Center for Microgravity and Materials Research at the University of Alabama in Huntsville.

[1] L. J. DeLucas and C. E. Bugg, Trends in Biotechnology **5**, 188 (1987); N. E. Chayen *et al.*, Q. Rev. Biophys. **29**, 2 (1996).

[2] P. Weber, in *Advances in Protein Chemistry*, edited by C. B. Afinsen, F. M. Richards, J. T. Edsal, and D. S. Eisenberg (Academic, New York, 1991), Vol. 41, p. 1; A. McPherson, J. Phys. D **26**, 104 (1993); Proceedings of the Fifth International Conference on Crystallization of Biological Macromolecules, edited by J. P. Glusker [Acta Crystallogr., Sect. D: Biol. Crystallogr. **D50**, 337 (1994)]; Proceedings of the Sixth International Conference on Crystallization of Biological Macromolecules, edited by K. Miki, M. Ataka, K. Fukuyama, Y. Higuchi, and S. Miyashita [J. Cryst. Growth **168**, 1 (1996)].

[3] L. A. Monaco and F. Rosenberger, J. Cryst. Growth **129**, 465 (1993), and references therein.

[4] V. Stojanoff, D. P. Siddons, L. A. Monaco, P. G. Vekilov, and F. Rosenberger, Acta Crystallogr., Sect. D: Biol. Crystallogr. **53**, 588 (1997).

[5] P. G. Vekilov and F. Rosenberger, J. Cryst. Growth **158**, 540 (1996), and references therein.

[6] P. G. Vekilov, L. A. Monaco, V. Stojanoff, B. R. Thomas, and F. Rosenberger, Acta Crystallogr., Sect. D: Biol. Crystallogr. **52**, 785 (1996).

[7] T. A. Land, A. J. Malkin, Yu. G. Kuznetsov, A. McPherson, and J. J. De Yoreo, Phys. Rev. Lett. **75**, 2774 (1995); A. J. Malkin, T. A. Land, Yu. G. Kuznetsov, A. McPherson, and J. J. De Yoreo, *ibid.* **75**, 2778 (1995).

[8] P. G. Vekilov, L. A. Monaco, and F. Rosenberger, J. Cryst. Growth **146**, 289 (1995).

[9] P. G. Vekilov, J. I. D. Alexander, and F. Rosenberger, Phys. Rev. E **54**, 6650 (1996).

[10] P. J. Ortoleva, *Geochemical Self-Organization* (Oxford University Press, New York, 1994); C. J. Allegré, A. Provost, and C. Jaupart, Nature (London) **294**, 223 (1981).

[11] J. M. Garcia-Ruiz, A. Santos, and E. J. Alfaro, J. Cryst. Growth **84**, 555 (1996), and references therein; R. I. Ristic, B. Shekunov, and J. N. Sherwood, *ibid.* **160**, 330 (1996).

[12] M. C. Cross and P. C. Hohenberg, Rev. Mod. Phys. **65**, 851 (1993); P. Gray and S. K. Scott, *Chemical Oscillations and Instabilities. Non-linear Chemical Kinetics* (Clarendon, Oxford, 1990); R. M. Noyes and R. J. Fields, Annu. Rev. Phys. Chem. **25**, 95 (1974).

[13] P. G. Vekilov, H. Lin, and F. Rosenberger, Phys. Rev. E **55**, 3202 (1997).

[14] E. Bauser, in *Handbook of Crystal Growth*, edited by D. Hurle (North-Holland, Amsterdam, 1994), Vol. 3b, p. 879.

[15] P. G. Vekilov and F. Rosenberger, J. Cryst. Growth (to be published).

[16] B. R. Thomas, P. G. Vekilov, and F. Rosenberger, Acta Crystallogr., Sect. D: Biol. Crystallogr. **D52**, 776 (1996).

[17] B. R. Thomas, P. G. Vekilov, and F. Rosenberger, Acta Crystallogr., Sect. D: Biol. Crystallogr. **D54**, 226 (1998).

[18] F. Rosenberger, P. G. Vekilov, H. Lin, and J. I. D. Alexander, Microgravity Sci. Technol. **10**, 29 (1997).

[19] P. G. Vekilov, B. R. Thomas, and F. Rosenberger, J. Phys. Chem. (to be published).

[20] P. G. Vekilov and F. Rosenberger, Phys. Rev. Lett. **80**, 2654 (1998).